TÜBİTAK

Turkish Journal of Physics

http://journals.tubitak.gov.tr/physics/

Research Article

Turk J Phys
(2022) 46: 155 – 161

doi:10.55730/1300-0101.2720

Investigating the potential of laser-written one-dimensional photonic crystals inside silicon

Onur TOKEL[1,2*]
[1]Department of Physics, Bilkent University, Ankara,Turkey
[2]National Nanotechnology Research Center, Ankara,Turkey

Received: 14.06.2022 • **Accepted/Published Online:** 15.08.2022 • **Final Version:** 31.08.2022

Abstract: The field of silicon photonics is based on introducing and exploiting advanced optical functionality. Current efforts in the field are based on conventional micro/nanofabrication methods, leading to optical functionality over wafer surfaces. A complementary and emerging field is introducing analogous optics directly within the wafer using lasers. Here we investigate the theoretical feasibility of a subclass of such optics, photonic crystals. Our efforts will guide future experimental efforts towards in-chip spectral control.

Keywords: Laser lithography, laser writing, 3D fabrication, optical gratings, silicon

1. Introduction

Silicon (Si) is one of the most important materials for modern technology, in particular for electronics and Si-photonics industries [1]. Virtually all Si-based applications, including hybrid systems rely on conventional fabrication approaches aiming to introduce and integrate functionalities over the wafer surfaces [2]. An emerging field is taking a complementary approach, which aims to relocate functionality form the chip surface to the bulk of the wafer. This approach exploits laser lithography [3], where laser pulses are nonlinearly absorbed within the material at a wavelength where it is transparent. The strong energy gradients created within the bulk induce subsurface disruptions without altering the wafer surface [3]. Once modifications form, it is also possible to convert them into optical elements by rearranging the optical index in three dimensions [4]. Analogous methods have been shown very successfully in other materials, including various crystals, glasses, polymers [5–7, 16].

The concept of creating subsurface structures with lasers is illustrated in Figure 1. Such buried structures are called in-chip or in-volume modifications. In the case of Si, modifying the bulk without altering the wafer surface had proved quite challenging, in earlier cases even impossible [8, 9]. The solution came from using nanosecond laser pulses in a regime where nonlinearities are designed to self-focus the laser beam in order to overcome the plasma shielding [3].

The freedom to control optical index within silicon already led to diverse applications, such as information storage [10], Fresnel zone plates [11], Fourier and Fresnel holograms [3], and type-I and type-II waveguides [12–14]. In addition, with an optional second step, selective chemical etching can be

*Correspondence: otokel@bilkent.edu.tr

used to remove the laser modified areas leading to high-volume covering 2D and 3D architectures [3]. We recently reviewed the emerging applications in detail [15]. The preceding advances so far focused on exerting control on the amplitude and phase of light in Si. Two exciting future directions are exerting spectral and polarisation control within the wafer using laser lithography. These capabilities, if realized, have the potential to create a complete photonics toolbox, with implications on integrated photonics [15]. Here, we explore the possibility of one-dimensional photonic crystals with input from experiments, in order to guide future efforts towards spectral control within the wafer.

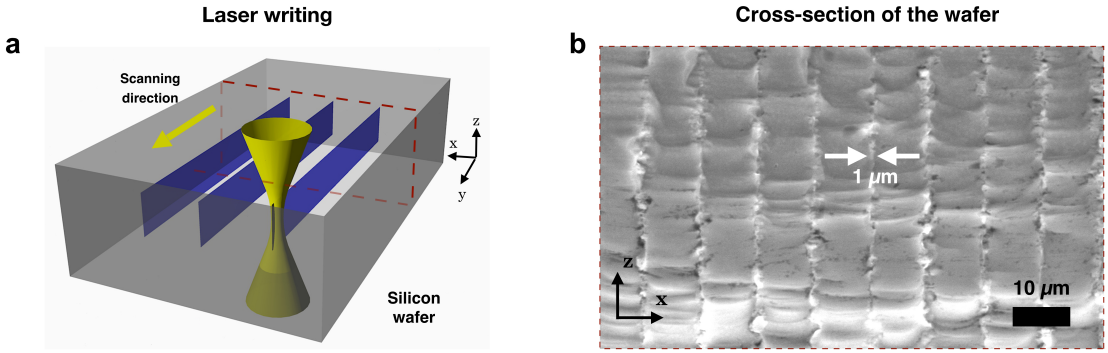

Figure 1. Fabrication of periodic structures in Si. (a) The conceptual illustration of laser-lithography. The laser propagates along the z axis, while the sample is scanned along y axis. The blue colored planes represent buried modifications. (b) Scanning electron microscope image of the wafer taken from the x-z plane after laser writing. Regular and periodic modifications are visible, extending parallel to the z axis. Scale bar: 10 μm.

The pattern that will form the basis of our analysis is illustrated in Figure 1. The details of the fabrication process is described in previous work [3]. Briefly, a linearly polarized laser of 8 ns pulse width, 1550 nm wavelength, 150 kHz repetition rate and $\approx$ 20 μJ pulse energy is focused within the wafer (Figure 1a). The sample is scanned along the y axis with a computer-controlled translation stage. After this step, the structures are characterized by dicing the wafer along $x-z$ plane, e.g., as shown with red dashed line in Figure 1a. Then, the sample can be imaged with scanning electron microscopy (Figure 1b). Here the vertical lines of $\approx$ 1 μm thickness indicate the subsurface modifications. They elongate over the z axis, i.e., along the laser propagation direction. In this representative case, their separation is chosen as 10 μm; nonetheless, this can be controlled with high accuracy using the translation stage. Thus, regular subsurface patterning with one dimensional periodicity is established.

It has been shown that the refractive index of the modified parts is different from that of the crystal matrix [3, 14]. Thus, when light is sent along the periodic index modulation (x axis), it would partially reflect from each interface. In such cases, one may expect to create resonances, i.e. a one dimensional photonic crystal [17], exploiting subsurface patterns. In the next section, we will outline the mathematical model used to analyze such optical behavior. Then, we will apply the model to lithographic patterns similar to Figure 1b, in order to explore their potential for spectral control.

2. Transfer matrix model

While a small number of reflections and transmissions are relatively simple to calculate, such as Fresnel reflections between two dielectric interfaces, the process rapidly becomes challenging to keep track of,

when the number of interfaces are high. For such cases, a powerful computational method is using the transfer matrix method (TMM)[17]. In its application to in-chip optical elements, we will assume that monochromatic coherent light impinges on a surface with normal incidence, as shown in Figure 2a. It will first propagate a distance of d_1 in the medium with refractive index n_1, and then impinge on the second medium of refractive index n_2. At this interface it will go through partial reflection. The transmitted component will continue a further distance of d_2 in the second medium. The combination of d_1 and d_2 will provide our unit matrix for the TMM. This unit will be called M_0 and is shown conceptually in Figure 2b. In the most general case, the next unit can be different, however since we assume periodic modulation of optical index along the optical axis, M_0 will be repeated N times.

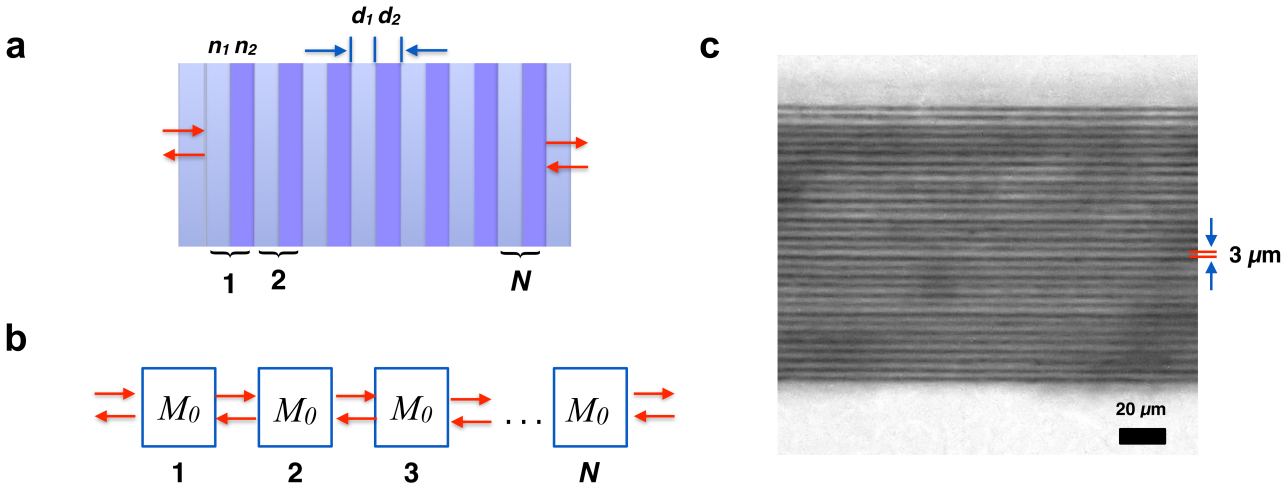

Figure 2. Transfer matrix method applied to in-chip optics. (a) Schematic representation of periodic index modulation. n_1 represents the refractive index of crystal silicon, n_2 represents the index for laser-written sections. (b) The conceptual representation of transfer matrix method with identical and repeating units. The corresponding transfer matrix for the unit is M_0. (c) Infrared transmission microscope image of a plane buried inside silicon. The dark lines correspond to modified areas, whereas the lighter color corresponds to crystal Si.

The details of the M_0 matrix describing the input-output relationship for the unit will depend on n_1, n_2, d_1 and d_2. We will later find the components of this matrix explicitly. However, with the simplifying assumption that the system is lossless and symmetric it will have the following form,

$$M_0 = \begin{bmatrix} 1/t^* & r/t \\ r^*/t^* & 1/t \end{bmatrix}. \tag{1}$$

Here t is the transmission amplitude and r is the reflection amplitude of the unit, respectively. Then, the total system is described by multiplying the M_0 matrix N times, i.e. M_0^N. The final matrix is then given as [17],

$$M_{total} = \Psi_N M_0 - \Psi_{N-1} I. \tag{2}$$

In the preceding equation, the Ψ_N term is $\Psi_N = \frac{\sin(N\Phi)}{\sin\Phi}$, where $\cos(\Phi) = Re(1/t)$. In order to find the power reflectance of the entire system, we need the reflection coefficient. This can be found

from the transfer matrix (M_{total}) of the N-segment system. Since the unit segment is assumed to be lossless and symmetric, the matrix of the entire system will also have the general form:

$$M_{total} = \begin{bmatrix} 1/t_N^* & r_N/t_N \\ r_N^*/t_N^* & 1/t_N \end{bmatrix}, \tag{3}$$

where t_N is the complex transmission amplitude and r_N is the complex reflection amplitude. Plugging Equations 1 and 3 into Equation 2 and solving provides the following equations:

$$1/t_N = \Psi_N(1/t) - \Psi_{N-1} \tag{4}$$

$$r_N/t_N = \Psi_N(r/t). \tag{5}$$

The power transmittance is $T_{total} = |t_N|^2$. The power reflectance can be found from energy conservation as $R_{total} = 1 - T_{total}$. Finally, the power reflectance is given as [17],

$$R_{total} = \frac{\Psi_N^2 R}{1 - R + \Psi_N^2 R}, \tag{6}$$

where $R = |r|^2$. We note that the total power reflectance depends on the components of M_0 through multiple terms. First, it depends on Ψ_N, which directly depends on t. Further, it depends on r in a highly nonlinear manner in our case, as will be shown next. However, once the terms of Equation 6 are explicitly found, we can analyze the spectral response of in-chip optics such as Figure 2c.

2.1. Transfer matrix of the unit cell

In order to calculate the M_0 matrix we need four matrices. The first one is the propagation in n_1 medium a distance of d_1 which will be represented with b matrix. The second one is the interface between n_1 and n_2, represented by matrix c. This is followed by the propagation in the n_2 medium a distance of d_2, which is represented with matrix d. Finally the interface from n_2 to n_1 is represented with the matrix e. These matrices can be calculated as follows:

$$b = \begin{bmatrix} exp(-i\phi_1) & 0 \\ 0 & exp(i\phi_1) \end{bmatrix},$$

$$c = \frac{1}{2n_2} \begin{bmatrix} n_2 + n_1 & n_2 - n_1 \\ n_2 - n_1 & n_2 + n_1 \end{bmatrix},$$

$$d = \begin{bmatrix} exp(-i\phi_2) & 0 \\ 0 & exp(i\phi_2) \end{bmatrix},$$

$$e = \frac{1}{2n_1} \begin{bmatrix} n_1 + n_2 & n_1 - n_2 \\ n_1 - n_2 & n_1 + n_2 \end{bmatrix},$$

where $\phi_1 = n_1.k_0.d_1$, $\phi_2 = n_2.k_0.d_2$; and $k_0 = 2\pi/\lambda_0$. Then, M_0 can be found as

$$M_0 = e.d.c.b \tag{7}$$

Equating Equation 7 to Equation 1 one can explicitly solve the matrix components of M_0. For instance, the complex transmission amplitude t relates to the refractive indices as follows:

$$\mathrm{Re}(1/t) = (n_1 + n_2)^2 \cos(\pi x)/(4n_1n_2) - (n_2 - n_1)^2 \cos(\xi \pi x)/(4n_1n_2), \tag{8}$$

where $\xi = (n_1.d_1 - n_2.d_2)/(n_1.d_1 + n_2.d_2)$, $x = \nu/\nu_B$, and $\nu_B = (2c/(n_1 + n_2))/2(d_1 + d_2)$. This last term, υ_B is also called the Bragg frequency, and we will later normalize the data to this value. Equation 8 can be used to calculate the Ψ_N term of Equation 6. The complex reflection amplitude r can be related to the refractive indices using $|r|^2 + |t|^2 = 1$. Finally, the $R = |r|^2$ relation can be used in Equation 6 to calculate R_{total}. In the next section, this approach will be implemented and R_{total} will be calculated for various in-chip optical components.

3. Simulation results and discussion

Refractive index engineering in Si is a field of active study. Thus, we will explore various scenarios with input from available experiments, with an eye towards pushing the fabrication limits. One scenario is crystal disruptions leading to amorphisation. This would correspond to an optical index of about 3.7, compared to the index of 3.5 of crystal silicon. We simulate such a scenario assuming $N = 50$, $n_1 = 3.5$, $n_2 = 3.7$. The dimensions are chosen similar to that of Figure 2c. The simulation solves Equation 6 for the preceding parameters (Figure 3a) with $d_1 = 1$ μm and $d_2 = 2.5$ μm for the blue curve, and $d_2 = 2.0$ μm for the red curve. We observed strong power reflectance at bands of resonances (stop bands) that are around integer multiples of the frequency ν_B. Such a case would correspond to an in-chip one-dimensional photonic crystal. We also observed that potential fabrication errors on the order of 500 nm can cause change in the spectral behavior for higher order bands.

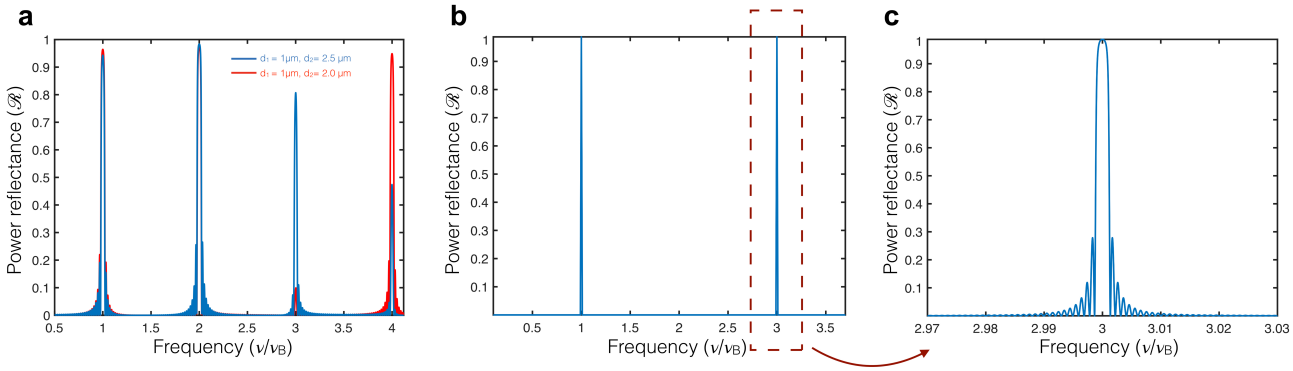

Figure 3. Simulation results for photonic crystals. (a) Power reflectance for $N = 50$, Δn $= 0.2$, $d_1 = 1$ μm, blue curve assumes $d_2 = 2.5$ μm; red curve assumes $d_2 = 2.0$ μm. (b) Power reflectance for $N = 1000$, Δn $= 0.01$, $d_1 = d_2 = 1$ μm. (c) The close-up view of a stop band.

Another scenario is to have partial crystal disruptions with an index contrast of about 0.01 [15]. Such a case is simulated with the following assumptions, $N = 1000$, Δn $= 0.01$, d_1=1 μm and d_2=1 μm. The corresponding power reflectance simulation is given in Figure 3b. Since the index contrast

is lower here, a larger N value is required in order to create complete resonances. The stop bands are observed around a narrow frequency range of odd-integer multiples of ν_B. A representative close-up view of the bands is given in Figure 3c. We find that in this scenario, it would still be possible to create photonic crystals, however qualitatively different filtering characteristics would be observed.

The significance of improving the resolution limit and side wall roughness is further highlighted with this work. The transparency window of silicon suggests that our technique may be applied for fabrication of photonic crystals in the infrared wavelength range, for instance 2 μm. Thus, one requires close to or better than 1-μm resolution, which is already attainable. Further, in order to attain low-loss optics, one would require precise fabrication over large volume ($\approx$ mm^3) preserving low surface roughness (e.g., $\lambda/10 = 200$ nm), in particular for cases requiring high N (e.g., $N = 1000$). While this will be experimentally challenging, early indications from our group strongly indicate the possibility. In particular, we recently showed the first in-chip laser nanofabrication with submicrometer roughness and pitch [18]. Further, our preliminary results indicate the possibility of selective chemical etching of laser-modified regions, which can potentially result in high-optical index contrast (air-Si). Such an advance would also remove the need for using high N, as only 10-20 layers would be needed to accumulate comparable phase.

4. Conclusion

In summary, we applied TMM to in-chip index gradients and found parameters that would be needed in order to create photonic crystals in Si. We found that the refractive index contrast that is already possible may be enough to create such optics, if one can create them with large numbers, e.g., with $N = 1000$. The main loss mechanism is expected to be scattering from side walls of modified parts, which could be significant for high N values. Hence, future efforts should also focus on increasing index contrast. This may be achieved with future advances leading to amorphisation, or potentially with selective chemical etching leading to void creation as shown in [3], albeit at lower scale.

We note that 3D architecture (i.e., form) is closely associated with the fabrication method. There is also a strong relationship between *form* and *function*. Thus, it is expected that diverse functionality to emerge from more complex geometries. While in this work we limited ourselves to micropatterning with 1D periodicity, using the large parameter space already available, which includes using longitudinal or transverse laser writing, nanosecond or femtosecond pulses, single pulse/multipulse writing, it should be possible to create a plethora of 3D patterns [15]. While the current features are limited to $\approx$ 1 μm, we expect intense efforts of the community to address the resolution related limits, significantly increasing available functionalities. Thus, advances in laser lithography along with support from simulations such as in this work will help advance the field.

Acknowledgment

We acknowledge support of Scientific and Technological Research Council of Turkey (TÜBİTAK) (project no: 121F387) and Turkish Academy of Sciences Young Investigator Program (TÜBA-GEBİP) Award.

References

[1] R. Soref, "Mid-infrared photonics in silicon and germanium," *Nature Photonics* **4** 8 (2010) 495–497.

[2] S. J. B. Yoo, B. Guan and R. P. Scott, "Heterogeneous 2D/3D photonic integrated microsystems," *Microsyst. Nanoeng.* **2** (2016) 16030–16039.

[3] O. Tokel, A. Turnalı, G. Makey, P. Elahi, T. Çolakoğlu, et al,"In-chip microstructures and photonic devices fabricated by nonlinear laser lithography deep inside silicon," *Nature Photon.* **11** (2017) 639–645.

[4] R. R. Gattass and E. Mazur, "Femtosecond laser micromachining in transparent materials," *Nature Photon.* **2** (2008) 219–225.

[5] T. Gissibl, S. Thiele, A. Herkommer, H. Giessen "Two-photon direct laser writing of ultracompact multi-lens objectives," *Nature Photon.* **10** (2016) 554–560.

[6] W. Yang, G.Kazansky, and Y. P. Svirko, "Non-reciprocal ultrafast laser writing," *Nature Photon.* **2** (2008) 99–104.

[7] K. Sugioka and Y. Cheng, "Femtosecond laser three-dimensional micro- and nanofabrication," *Appl. Phys. Rev.* **1** (2014) 041303-1–041303-35.

[8] D. Grojo, A. Mouskeftaras, P. Delaporte and S. Lei, "Limitations to laser machining of silicon using femtosecond micro-Bessel beams in the infrared," *J. Appl. Phys* **117** (2015) 153105-1–153109-7.

[9] V. V. Kononenko, V. V. Konov and E. M. Dianov, "Delocalization of femtosecond radiation in silicon," *Opt. Lett.* **37** (2012) 3369–3371.

[10] O. Tokel, I. Pavlov, I. Akca, S. Tozburun, A. Turnali and F. Ö. Ilday, "Laser-writing in silicon for 3D information processing, (2014)," `arXiv:physics.optics:1409.2827`.

[11] A. Turnali, O. Tokel, I. Pavlov and F. Ö. Ilday, "Direct laser writing of volume fresnel zone plates in silicon", (2015), *European Conference on Lasers and Electro-Optics - CLEO* **CM-4-5** (2015).

[12] I. Pavlov, O. Tokel, S. Pavlova, V. Kadan, G. Makey et al, "Femtosecond laser written waveguides deep inside silicon," *Opt. Lett.* **42** (2017) 3028–3031.

[13] M. Chambonneau, Q. Li, M. Chanal, N. Sanner, and D. Grojo, "Writing waveguides inside monolithic crystalline silicon with nanosecond laser pulses, (2017)," *Opt. Lett.* **41** (2016) 4875–4878.

[14] A. Turnali, M. Han and O. Tokel, "Laser-written depressed-cladding waveguides deep inside bulk silicon," *Opt. Lett.* **36** (2019) 966–970.

[15] M. Chambonneau, D. Grojo, O. Tokel, F. Ö. Ilday, S. Tzortzakis and S. Nolte, "In-volume laser direct writing of silicon-challenges and opportunities," *Lasers Photon. Rev.* **15** 11 (2021) 2100140-1–2100140-35.

[16] A. Ródenas, M. Gu, G. Corrielli, P. Paié, S. John, A. K. Kar and R. Osellame, "Three-dimensional femtosecond laser nanolithography of crystals," *Nature Photon.* **13** (2019) 105–109.

[17] B. E. A. Saleh and M. C. Teich, "Fundamentals of photonics," *John Wiley and Sons, Inc* (1991).

[18] O. Tokel, "Laser nanofabrication buried deep inside silicon wafers," *SPIE Photonics West* San Fransisco (2022).